



ULUSLARARASI 3B YAZICI TEKNOLOJİLERİ
VE DİJİTAL ENDÜSTRİ DERGİSİ

INTERNATIONAL JOURNAL OF 3D PRINTING
TECHNOLOGIES AND DIGITAL INDUSTRY

ISSN:2602-3350 (Online)

URL: <https://dergipark.org.tr/ij3dptdi>

EFFECT OF GEOMETRIC MODIFICATIONS ON THE COMPRESSIVE STRENGTH AND MECHANICAL PERFORMANCE OF GYROID- BASED BONE SCAFFOLDS

Yazarlar (Authors): Muhammet Mevlüt Karaca *, İzel Ekinci , Daver Ali 

Bu makaleye şu şekilde atıfta bulunabilirsiniz (To cite to this article): Karaca M. M., Ekinci İ., Ali D., “Effect of Geometric Modifications on the Compressive Strength and Mechanical Performance of Gyroid-Based Bone Scaffolds” *Int. J. of 3D Printing Tech. Dig. Ind.*, 9(1): 63-72, (2025).

DOI: 10.46519/ij3dptdi.1609933

Araştırma Makale/ Research Article

Erişim Linki: (To link to this article): <https://dergipark.org.tr/en/pub/ij3dptdi/archive>

EFFECT OF GEOMETRIC MODIFICATIONS ON THE COMPRESSIVE STRENGTH AND MECHANICAL PERFORMANCE OF GYROID-BASED BONE SCAFFOLDS

Muhammet Mevlüt Karaca^{a*} , İzel Ekinci^b , Daver Ali^b 

^aKarabuk University, Engineering Faculty, Mechanical Engineering Department, KARABUK

^bKarabuk University, Engineering Faculty, Biomedical Engineering Department, KARABUK

* Corresponding Author: mmevlutkaraca@karabuk.edu.tr

(Received: 30.12.24; Revised: 08.03.25; Accepted: 15.03.25)

ABSTRACT

Porous structures are of great interest in biomedical and engineering applications due to their light weight, high mechanical strength, and biological compatibility. In this study, based on the widespread use of gyroid structures in bone scaffolds and their potential to adapt to the heterogeneous mechanical properties of bone tissue, the effect of geometric arrangements on mechanical strength was investigated. Using the tri-periodic minimal surface trigonometric function, the reference model G(0) with 80% porosity was taken as a basis, and three different geometries were created by reducing the unit cell of the gyroid on the y-axis by 25% (G(-25)), keeping it constant (G(0)), and enlarging it by 25% (G(+25)). Using the biomaterial PLA, these non-isotropic structures were fabricated through Fused Deposition Modeling (FDM) and 3D printed in the longitudinal and lateral axes, then subjected to compression tests. The compression test results showed that the printing direction and loading direction play a decisive role in mechanical strength. Especially when the printing and loading directions were the same, an increase in strength was observed, with the G(-25) model exhibiting 37.8% higher strength than G(0) in the PLt-CLt (Printed Lateral – Compression Lateral) configuration. Conversely, increasing the pore size resulted in a 14.7% reduction in strength for G(-25) compared to G(0). Furthermore, when the printing and loading directions were aligned, the lateral axis exhibited 38.4% higher strength than the longitudinal axis in the G(-25) model. It was found that the arrangement of the pores parallel to the load direction minimized strength loss, and the increase in porosity did not significantly affect mechanical strength. In addition, the structure of the compression layers before and after the test was examined in detail by SEM analysis. The findings show that the geometrical arrangements of the gyroid structures have a significant effect on mechanical strength and that these structures can be optimized and used in biomedical applications.

Keywords: FDM, PLA, Gyroid Structure, Porosity, Bone Scaffold, Anisotropic Structure.

1. INTRODUCTION

Porous structures are of great interest in biomedical and engineering applications due to their properties such as light weight, high mechanical strength and biocompatibility. In particular, Triply Periodic Minimal Surface (TPMS) have become an important focus for scaffold design in biomedical applications. The unique geometric properties of TPMS structures allow them to mimic the mechanical behavior of natural bone, making them promising candidates for bone tissue engineering [1-2]. These surfaces are characterized by zero mean curvature, high surface-to-volume ratio, and

interconnected porous structure, and offer a favorable environment for bone regeneration by promoting cell adhesion and proliferation [3-4]. Gyroid structures represent an important subgroup of TPMS and are widely used in tissue engineering, implant design and other biomedical applications. Their interconnected porous network facilitates essential biological processes such as cell infiltration, vascularization, and nutrient transport, which are critical for the regeneration of both bone and soft tissues. These properties enhance osteointegration by promoting osteoblast adhesion and proliferation, ultimately

improving implant stability [5-6]. Furthermore, studies indicate that gyroid scaffolds provide a more uniform stress distribution compared to conventional strut-based lattice structures, leading to enhanced mechanical performance and reduced stress concentrations [7-8]. Gyroid structures offer an ideal option for load-bearing implants due to their unique mechanical performance and biocompatibility. For example, Eltlhawy et al. [9] demonstrated that gyroid cellular titanium is compatible with the mechanical properties of human bone and exhibits a 70% stiffness reduction, increasing the potential for successful integration in orthopedic applications. Pore size and porosity also significantly affect the performance of these structures. In the same study, a pore size of 500 μm and a porosity of approximately 77% were reported to promote bone growth and increase bone-implant fixation stability. The advantages of gyroid structures in terms of stress distribution are noted for their lower stress concentrations compared to conventional support-based lattice structures. Hayashi et al. [8] showed that stress distribution in gyroid scaffolds is more homogeneous and that these structures outperform conventional scaffolds in terms of both strength and bone regeneration capabilities. In Ali's study [10], it was shown that the anisotropic properties of gyroid structures adapt to the mechanical and biological behavior of the bone structure. In the study, elastic modulus and permeability analyses were performed on gyroid scaffolds designed using different geometric variations and it was determined that these structures exhibit bone-like properties. The energy absorption capacity of gyroid structures is also superior to other porous structures. Hayashi et al. [8] determined that gyroid structures exhibit three times more specific energy absorption under pressure compared to other lattice structures.

The role of porosity and pore size in the design of gyroid and similar scaffolds is critical. Pore sizes have direct effects on cell infiltration, nutrient transport and mechanical strength [11-12]. Naghavi et al. [13] showed that gyroid structures with porosity between 52% and 66% exhibited hardness (4-5.8 GPa) and yield strength (120-225 MPa) similar to cortical bone. This was confirmed by Musthafa's study [14], which showed that structures with pore sizes smaller than 800 μ can offer mechanical

properties in the range of cortical bone. When the effect of pore size on mechanical strength was examined, Wu et al. [15] reported that smaller pore sizes increase compressive strength and there is an inverse relationship between pore size and mechanical strength. Caiazzo et al. [16] showed that the mechanical properties of Gyroid structures can be tuned by varying unit cell sizes and porosity ratios, thus optimizing the elastic modulus and compressive strength.

The mechanical properties of additively manufactured lattice structures show significant changes depending on parameters such as unit cell size and loading direction. For example, when the unit cell size is increased from 2 mm to 8 mm in 316L stainless steel gyroid lattice structures, the yield strength and elastic modulus decrease by 63.43% and 63.74%, respectively [17]. Similarly, the compressive modulus and compressive strength decrease by 10.33% and 29.45%, respectively [18]. Significant differences were also observed depending on the loading direction, and the elastic modulus of gyroid trusses produced in perpendicular direction was found to be 22.95% higher than those produced in parallel direction [17]. These data show that unit cell size and loading direction play a critical role in the design process of lattice structures and the mechanical properties should be optimized according to the targeted application.

Cellular structures are essential in engineering and biomedical applications due to their high specific strength, energy absorption capacity, and material efficiency [19]. TPMS structures ensure homogeneous stress distribution and superior mechanical performance, offering advantages over traditional lattices [18-19]. Conventional manufacturing methods are inadequate for producing such complex geometries, whereas additive manufacturing (AM) optimizes material usage, reduces production time, and minimizes waste. Among AM techniques, Selective Laser Melting (SLM) and Fused Deposition Modeling (FDM) excel in fabricating intricate cellular architectures with precise control over porosity and mechanical properties [18]. These advancements expand applications in aerospace, biomedical, and automotive industries.

In this study, the reference model G(0) was designed with a constant porosity of 80%, and three different geometries were obtained by reducing the unit cell of the gyroid structure on one axis by 25% (G(-25)), keeping it constant (G(0)) and enlarging it by 25% (G(+25)). The structures were 3D printed in two different directions in the longitudinal and lateral axes using the biomaterial Polylactic acid (PLA) and subjected to compression tests. The effect of printing direction, loading direction and porosity orientation on the mechanical properties of the obtained models were investigated. In addition, Scanning Electron Microscopy (SEM) images of the samples were taken after the mechanical tests and the adhesion and delamination between the printing layers were examined.

2. MATERIALS AND METHODS

2.1. Modeling and Geometric Structure

The basic surfaces of the skeletons were designed using the program K3Dsurf (k3dsurf.sourceforge.net). This design is based on the trigonometric function $\cos(x) \sin(\alpha y) +$

$\cos(\alpha y) \sin(z) + \cos(z) \sin(x) = 0$. For each model, the unit cells were repeated four times on three axes (x, y and z) to obtain a cube structure with a total of 64-unit cells. Information about the model unit cells and geometric parameters are given in Figure 1 and Table 1. The unit cell length was obtained in x, y, z on the boundary $[-\pi, \pi]$. For the models with scaling coefficients defined as -25%, 0% and 25%, α values were set as 0.75, 1 and 1.25, respectively. These models are named G(-25), G(0) and G(+25) according to the scaling percentage. SolidWorks software was used to thicken the surfaces and create solid models. The thickness of the scaffold walls was determined as 400 μm , and these structures were fabricated using Fused Deposition Modeling (FDM), a widely used additive manufacturing technique. FDM was chosen due to its capability to produce complex porous structures with high accuracy using PLA material. These structures can be easily manufactured with additive manufacturing technologies [20].

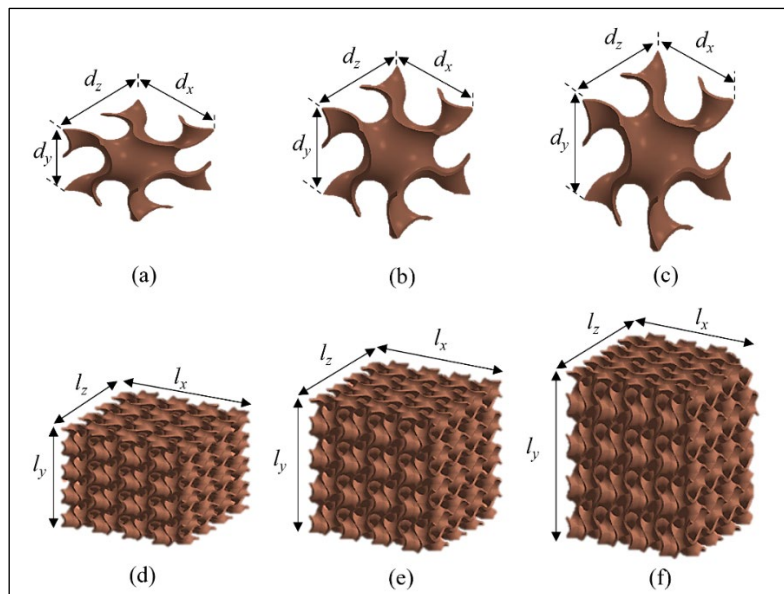


Figure 1. Unit cells of the designed gyroid structures: (a) G(-25), (b) G(0), (c) G(+25); full models: (d) G(-25), (e) G(0), (f) G(+25).

Table 1. Dimensions of the unit cell and the corresponding scaffold model (mm).

	Model		
Dimensions	G(-25)	G(0)	G(+25)
dx and dz	6,20	6,20	6,20
dy	4,58	6,20	7,72
Lx and Lz	25,54	25,55	25,33
Ly	19,09	25,32	31,54

2.2. Production of Samples

In this study, PLA filament was chosen for sample production due to its biocompatibility, biodegradability, and non-toxic degradation products. Widely used in scaffolds, drug delivery, and tissue engineering, PLA supports cell adhesion and reduces inflammation, as

shown in both in vitro and in vivo studies [21-23]. The properties of the Flashforge PLA Pro filament are listed in Table 2.

Table 2. Mechanical and physical properties of PLA Pro filament used [24].

Property	Test Method	Units	Typical Value
Density	ISO 1183	g/cm ³	1.25~1.26
Tensile Strength	ISO 527	MPa	45.5~49
Elongation at Break	ISO 527	%	14.5~16.5
Modulus of Elasticity	ISO 527	MPa	950~1050
Izod Impact Strength	ISO 180	KJ/m ²	9.5~10.5

The samples were produced using the Flash Forge Creator 3 Pro printer in accordance with the parameters specified in Table 3.

Table 3. Printing Parameters.

Parameters	Flash Forge - Creator 3 Pro
Material	PLA
Nozzle Diameter	0,4 mm
Printing Precision	0,1 mm
Extruder Temperature	210 °C
Bed Temperature	60 °C
Infill Density	% 100
Layer Thickness	0,18 mm
Print Speed	60 mm/s
Infill Pattern	Lines
Number of Wall Lines	3

In order to evaluate the effect of printing direction on mechanical properties, the specimens were printed in two different axes. As shown in Figure 2, the designed specimens were first printed in the longitudinal axis, then rotated 90° around the y-axis and printed in the lateral axis.

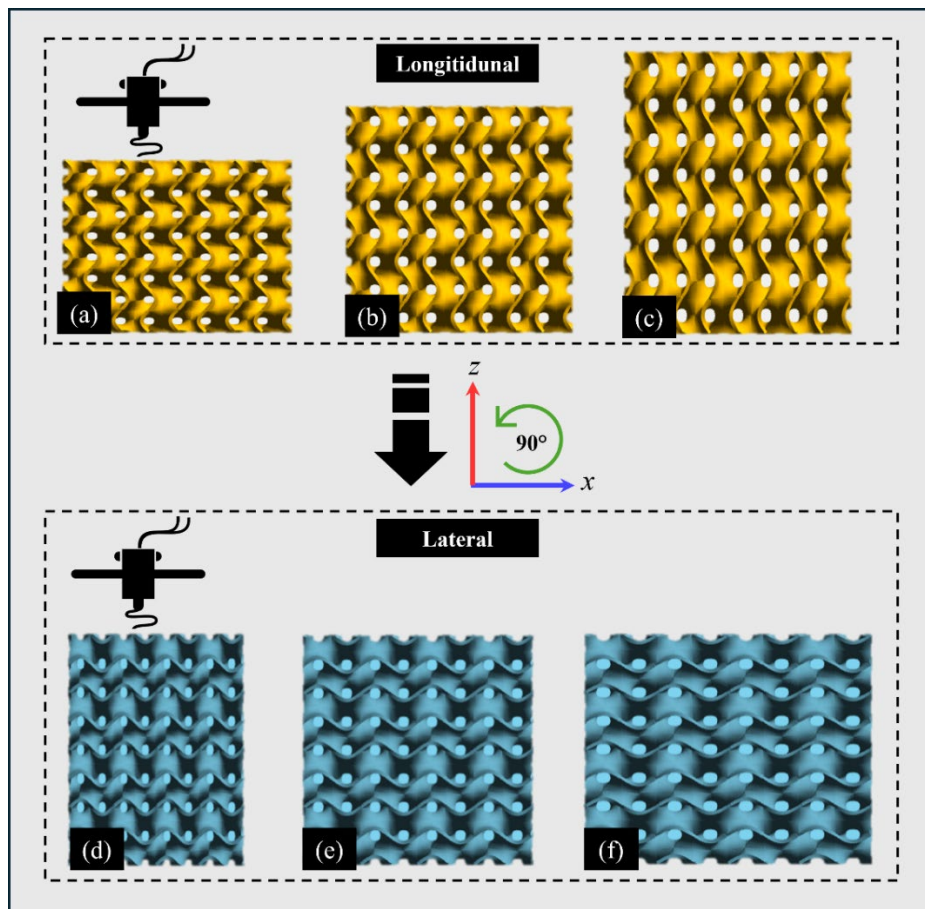


Figure 2. Gyroid structures produced in the longitudinal compression direction: (a) G(-25), (b) G(0) and (c) G(+25). Gyroid structures produced in the lateral compression direction: (d) G(-25), (e) G(0) and (f) G(+25).

2.3. Experimental Studies

Compression tests were performed on the successfully manufactured specimens. The sample specimens produced in the lateral direction are shown in Figure 3(a). The compression tests were conducted using a Zwick Z600 (Figure 3(b)) testing machine, with the test speed set to 2 mm/min in accordance with the ISO 604 standard. During the test, a deformation of 5 mm was applied to the specimens. Before and after the compression test, the structure of the specimens was examined by SEM. During the examinations, low levels of filamentation and porosity formation were observed in some areas, but it was observed that these formations were not significant and were not at a density that would adversely affect the mechanical performance. In addition, there was no visible delamination between the printing layers as a result of printing or detectable by SEM (Figure 3(c) and Figure 3(d)).

Analysis of the post-compression images revealed that the observed fracture behavior was

predominantly planar, with failure occurring along planes parallel to the compression direction. The narrowing effect observed under loading, as indicated in Figure 3(b), suggests localized stress concentrations that led to structural failure along these planes. The schematic representation within the figure further illustrates the deformation mechanism, showing that structural collapse primarily followed the interconnected porous architecture of the gyroid structure. No significant orthogonal fractures were detected, as no cracks propagating perpendicularly to the compression axis were observed.

The stringing behavior can be affected by printing parameters such as nozzle temperature, print speed and retraction settings. To solve this problem, strategies such as decreasing the nozzle temperature, increasing the printing speed and optimizing the retraction settings have been proposed [25-27].

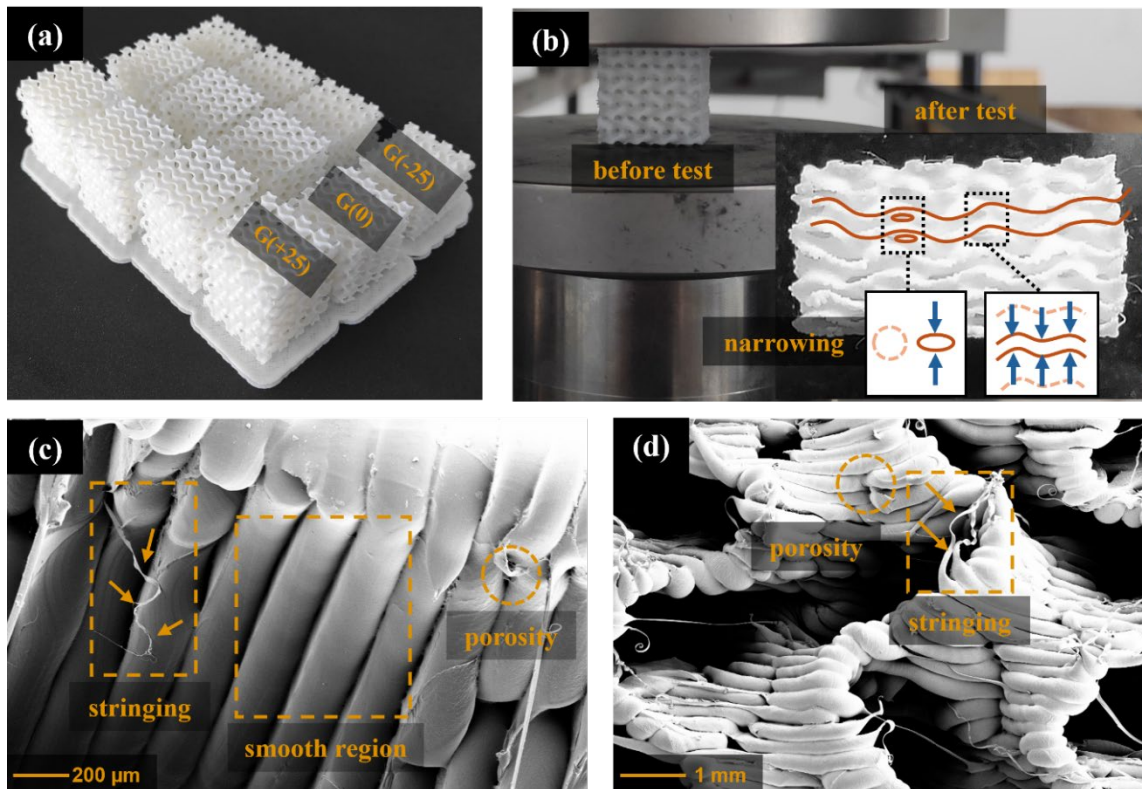


Figure 3. (a) 3D printed G(-25), G(0) and G(+25) samples, (b) Compression test of the gyroid scaffold samples before and after loading, (c) 200 µm scale SEM image, (d) 1 mm scale SEM image.

The compression test result graphs are given in Figure 4. The graphs compare the engineering stress-strain behavior (Figures 4a-4d), ultimate

compressive strength (Figure 4e) and deformation at maximum force (Figure 4f) of gyroid specimens of three different structures

(G(-25), G(0), G(+25)) under compression (PLo: Printed Longitudinal, PLt: Printed Lateral) and loading (CLo: Compression Longitudinal, CLt: Compression Lateral) conditions in different directions.

In Figures 4a and 4c, G(+25) specimens exhibited higher yield strength and ultimate compressive strength under PLo-CLo and PLa-CLt conditions, followed by G(0) and G(-25), respectively. Figure 4b and Figure 4d show that G(-25) specimens exhibited higher yield strength and ultimate compressive strength, followed by G(0) and G(+25), respectively.

According to Figure 4e, the highest ultimate compressive strength was observed in the PLt-

CLt G(-25) sample. This result was followed by PLo-CLo G(+25) and PLo-CLo G(0) samples, respectively. These findings reveal that when the printing direction and the test direction are the same, the material shows higher strength compared to other conditions. Similar results have been reported in the literature. Studies show that mechanical properties such as tensile, compressive and flexural strength increase significantly when the loading occurs in the same direction as the compression direction[28-31].

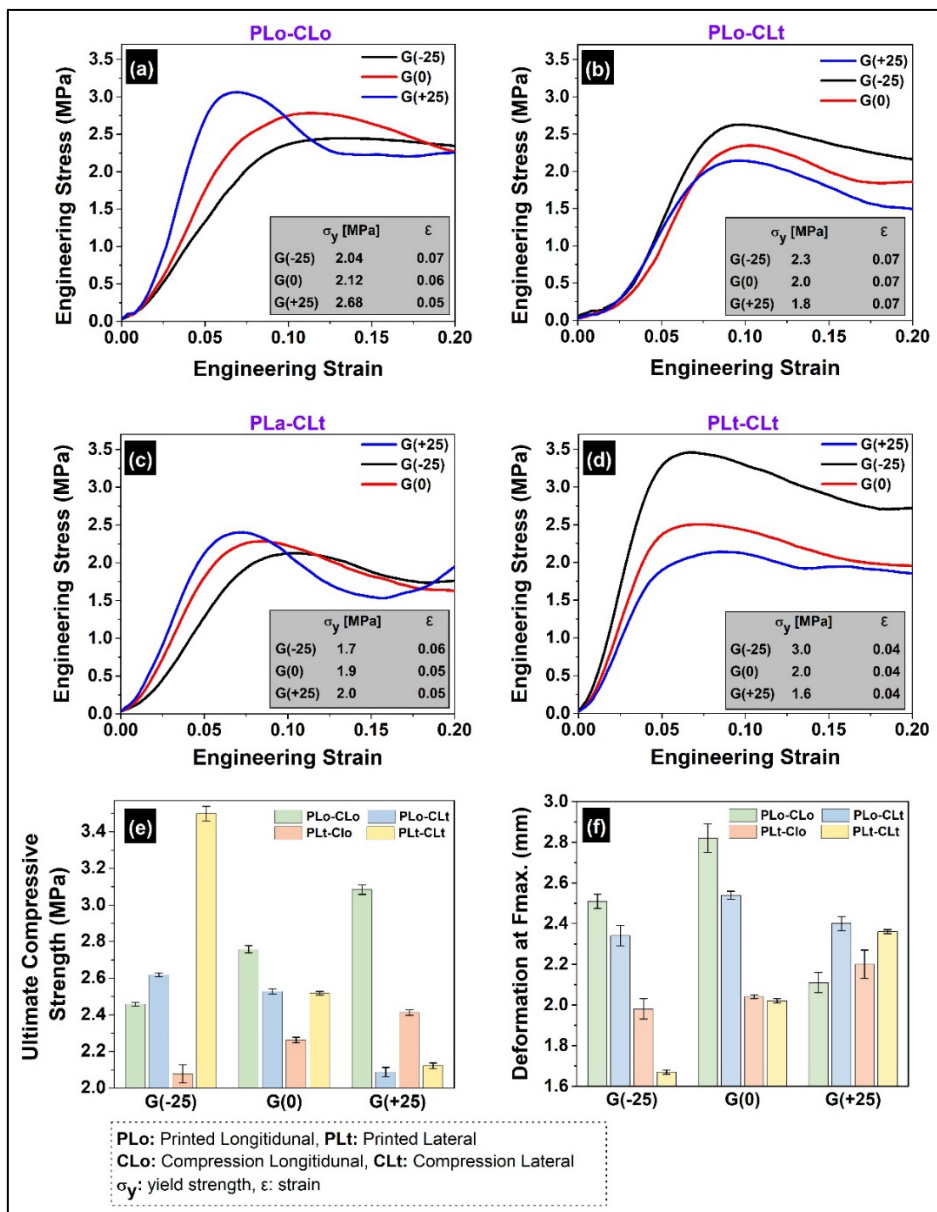


Figure 4. Engineering stress-strain curves and mechanical properties of compression tests at different compression and loading directions: (a) PLo-CLo, (b) PLo-CLt, (c) PLa-CLo, (d) stress-strain curves for PLa-CLt cases, (e) Ultimate compressive strength and (f) Deformation values at maximum force.

When PLt-CLt and PLo-CLt specimens are examined in Figures 4(b) and 4(d), the highest strength was observed at G(-25), followed by G(0) and G(+25), respectively. This is in line with the literature and can be explained by the effect of porosity on mechanical strength. The decrease in porosity improved the mechanical properties [32-33]. However, this result was reversed in PLo-CLo and PLt-CLo specimens. The probable reason for this is that the parallel arrangement of the pores to the load direction minimizes the strength loss and the increase in pores does not significantly affect the mechanical strength since the load carrying paths are not completely broken. Figure 5 shows the porosity distribution and dimensions of the specimens in the longitudinal and lateral directions. In the longitudinal direction, the width of the pores remained constant while the size of the pores changed. In the lateral direction, the heights of the pores are constant and the widths change. When these changes were analyzed, it was observed that the porosity widths in the longitudinal direction remained constant and were 1.16 mm. However, there were differences in the height values; the height

was measured as 0.78 mm for the G(-25) model, 1.16 mm for the G(0) model and 1.56 mm for the G(+25) model. In the lateral direction, the height values remained constant and were determined as 1.16 units. On the other hand, the width values changed and were measured as 0.78 mm for the G(-25) model, 1.16 mm for the G(0) model and 1.56 mm for the G(+25) model. Similar studies have shown that the mechanical strength of the material is higher when the pores are arranged parallel to the load direction. This is because the pores do not completely break the load carrying paths and minimize the strength loss[34-36]. In this case, the increase in porosity does not significantly affect the mechanical strength. On the other hand, in alignments perpendicular to the load direction, the pores interfere with load transfer and cause a decrease in strength. These findings indicate that pore orientation and loading direction play an important role in the mechanical properties of the material. In general, structure orientation and compression direction in scaffolds lead to significant differences in mechanical strength and deformation behavior.

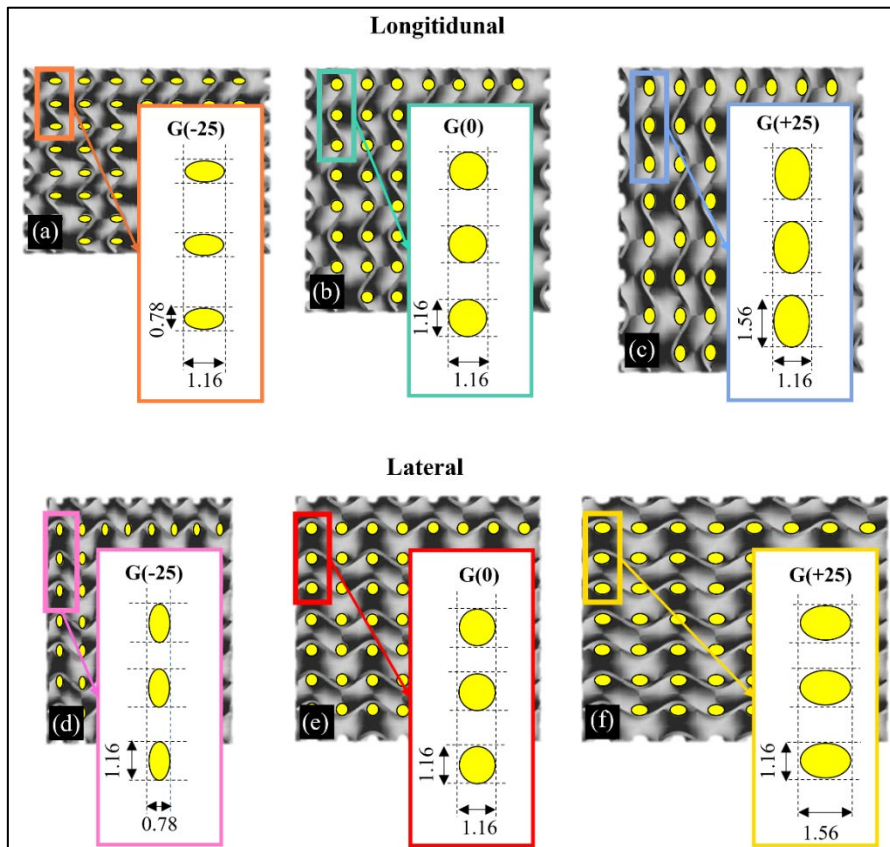


Figure 5. Pore shape and size of the specimens (mm): Longitudinal direction (a) G(-25), (b) G(0) and (c) G(+25); Lateral direction (d) G(-25), (e) G(0) and (f) G(+25).

3. CONCLUSIONS

In this study, the effect of geometric variations and compression-loading directions on the mechanical strength of gyroid structures is investigated in detail. Taking the G(0) model with constant 80% porosity as a reference, three different geometries with 25% reduction (G(-25)) and 25% enlargement (G(+25)) of the unit cell on the y-axis were evaluated. The findings are summarized as follows:

- Strength increased when the compression direction and loading direction were the same: Overlapping the loading direction with the compression direction improved the load carrying capacity by increasing the interlayer integrity. The G(-25) geometry showed the highest strength in the longitudinal direction.
- The strength differed in the longitudinal and lateral axes: Specimens produced in the longitudinal direction exhibited higher strength than those produced in the lateral direction due to the alignment of the filaments in the load direction.
- The reduction in pore size increased the mechanical strength: Smaller pore sizes improved the strength by making deformation of the scaffold structure more difficult. The G(-25) geometry therefore provided the best performance.
- The alignment of the pores parallel to the load direction improved the strength: Alignment of the pores parallel to the load direction minimized the strength loss, while alignment perpendicular to the load direction resulted in a decrease in mechanical strength.

In conclusion, this study revealed that geometrical optimization of gyroid structures, compression-loading directions and pore distribution significantly affect the mechanical strength. The usability of these structures in biomedical applications such as bone tissue engineering can be enhanced by accurately optimizing the geometric parameters. The results of this study further emphasize that

gyroid and similar architectural scaffolds are good alternatives for non-isometric bone.

ACKNOWLEDGMENTS

This research received funding from the Scientific and Technological Research Council of Turkey (TUBITAK) under the project number 124M262. The study was conducted in the laboratories of Karabuk University, Material Research and Development Centre, with their support gratefully acknowledged.

REFERENCES

1. Lehder, E. F., Ashcroft, I. A., Wildman, R. D., Ruiz-Cantu, L. A., and Maskery, I., "A multiscale optimisation method for bone growth scaffolds based on triply periodic minimal surfaces", *Biomechanics and Modeling in Mechanobiology*, Vol. 20, Issue 6, 2085-2096, 2021.
2. Zhang, Q., Ma, L., Ji, X., He, Y., Cui, Y., Liu, X., Xuan, C., Wang, Z., Yang, W., Chai, M., and Shi, X., "High-Strength Hydroxyapatite Scaffolds with Minimal Surface Macrostructures for Load-Bearing Bone Regeneration", *Advanced Functional Materials*, Vol. 32, Issue 33, 2022.
3. Noroozi, R., Shamekhi, M. A., Mahmoudi, R., Zolfagharian, A., Asgari, F., Mousavizadeh, A., Bodaghi, M., Hadi, A., and Haghhighipour, "In vitro static and dynamic cell culture study of novel bone scaffolds based on 3D-printed PLA and cell-laden alginate hydrogel", *Biomedical Materials*, Vol. 17, Issue 4, 2022.
4. Wang, Z., Liao, B., Liu, Y., Liao, Y., Zhou, Y., and Li, W., "Influence of structural parameters of 3D-printed triply periodic minimal surface gyroid porous scaffolds on compression performance, cell response, and bone regeneration", *Journal of Biomedical Materials Research Part B*, Vol. 112, Issue 1, 2024.
5. Charbonnier, B., Manassero, M., Bourguignon, M., Decambron, A., El-Hafci, H., Morin, C., Leon D., Bensedoum M., Corsia, S., Petite H., Marchat D., Potier, E., "Custom-made macroporous bioceramic implants based on triply-periodic minimal surfaces for bone defects in load-bearing sites", *Acta Biomaterialia*, Vol. 109, 254-266, 2020.
6. Verisqa, F., Park, J. H., Mandakhbayar, N., Cha, J. R., Nguyen, L., Kim, H. W., Knowles, J. C., "In vivo osteogenic and angiogenic properties of a 3d-printed isosorbide-based gyroid scaffold manufactured via digital light processing", *Biomedicines*, Vol. 12, Issue 3, 1-15, 2024.

7. Baumer, V., Isaacson, N., Kanakamedala, S., McGee, D., Kaze, I., Prawel, D. A., “Comparing ceramic fischer-koch-s and gyroid tpms scaffolds for potential in bone tissue engineering”, *Frontiers in Bioengineering and Biotechnology*, Vol. 12, 1-13, 2024.
8. Hayashi, K., Kishida, R., Tsuchiya, A., & Ishikawa, K., “Periodic Minimal Surface Gyroid Structure to Strut-Based Grid Structure in Both Strength and Bone Regeneration”, *ACS Applied Materials & Interfaces*, Vol. 15, Issue 29, 34570-34577, 2023.
9. Elthawy, B., “Numerical Evaluation of a Porous Tibial-Knee Implant using Gyroid Structure”, *Journal of Biomedical Physics and Engineering*, Vol. 12, Issue 1, 75-82, 2022.
10. Ali, D., “Mimicking Bone Anisotropic Structure with Modified Gyroid Scaffolds; A Finite Element Analysis”, *Politeknik Dergisi*, Vol. 24, Issue 4, 1637-1646, 2021.
11. Baumer, V., Gunn, E., Riegle, V., Bailey, C., Shonkwiler, C., and Prawel, D., “Robocasting of Ceramic Fischer–Koch S Scaffolds for Bone Tissue Engineering”, *Journal of Functional Biomaterials*, Vol. 14, Issue 5, 1-20, 2023.
12. Cubo-Mateo, N., and Rodríguez-Lorenzo, L. M., “Design of Thermoplastic 3D-Printed Scaffolds for Bone Tissue Engineering: Influence of Parameters of “Hidden” Importance in the Physical Properties of Scaffolds”, *Polymers*, Vol. 12, Issue 7, 1-14, 2020.
13. Naghavi, S. A., Tamaddon, M., Marghoub, A., Wang, K., Babamiri, B. B., Hazeli, K., Xu, W., Lu, X., Sun, C., Wang, L., Moazen, M., Wang, L., Li, D., and Liu, C., “Mechanical Characterisation and Numerical Modelling of TPMS-Based Gyroid and Diamond Ti6Al4V Scaffolds for Bone Implants: An Integrated Approach for Translational Consideration”, *Bioengineering*, Vol. 9, Issue 10, 1-25, 2022.
14. N. Musthafa, H.-S., Walker, J., Rahman, T., Bjørkum, A., Mustafa, K., & Velauthapillai, D., “In-Silico Prediction of Mechanical Behaviour of Uniform Gyroid Scaffolds Affected by Its Design Parameters for Bone Tissue Engineering Applications”, *Computation*, Vol. 11, Issue 9, 1-28, 2023.
15. Wu, F., Yang, J., Ke, X., Ye, S., Bao, Z., Yang, X., Zhong, C., Shen, M., Xu, S., Zhang, L., Gou, Z., and Yang, G., “Integrating pore architectures to evaluate vascularization efficacy in silicate-based bioceramic scaffolds”, *Regenerative Biomaterials*, Vol. 9, 1-10, 2022.
16. Caiazza, F., Alfieri, V., Guillen, D. G., and Fabbriatore, A., “Metal functionally graded gyroids: additive manufacturing, mechanical properties, and simulation”, *The International Journal of Advanced Manufacturing Technology*, Vol. 123, Issue 7-8, 2501-2518, 2022.
17. Gülcan, O., “Eklemeli İmalatla Üretilen Kafes Yapıların Mekanik Özellikleri Üzerine Etki Eden Faktörler”, *Makina Tasarım ve İmalat Dergisi*, Vol. 19, Issue 2, 64-81, 2021.
18. Ergene B, Yalçın B, “Eriyik yığıma modelleme (EYM) ile üretilen çeşitli hücresel yapıların mekanik performanslarının incelenmesi”, *Gazi Üniversitesi Mühendislik Mimarlık Fakültesi Dergisi*, Vol. 38, Issue 1, 201-217, 2023.
19. Khan, N., Riccio, A., “A systematic review of design for additive manufacturing of aerospace lattice structures: Current trends and future directions”, *Progress in Aerospace Sciences*, Vol. 149, 1-34, 2024.
20. Burkhard, M., Fünrstahl, P., and Farshad, M., “Three-dimensionally printed vertebrae with different bone densities for surgical training”, *European Spine Journal*, Vol. 28, Issue 4, 798-806, 2019.
21. Li, N., and Chen, J., “Advances in chemical modifications of polylactide biodegradable materials”, *3rd International Forum on Energy, Environment Science and Materials (IFEESM 2017)*, 1640-1643, Shenzhen, 2017.
22. Gonçalves, A. P. B., Barbosa, W. T., Vieira J. L., Barbosa, J. D. V., and Soares, M. B. P., “Production of the Scaffold Using 3D Bioprinting Applied to the Biomedical Area: A Bibliometric Study”, *Journal of Bioengineering, Technologies and Health*, Vol. 6, Issue 3, 244-251, 2023.
23. Shasteen, C., and Choy, Y. Bin., “Controlling degradation rate of poly(lactic acid) for its biomedical applications”, *Biomedical Engineering Letters*, Vol. 1, Issue 3, 163-167, 2011.
24. Flash Forge, “Technical Data Sheet”, https://after-support.flashforge.jp/uploads/datasheet/tds/PLA_Pro_TDS_EN.pdf, February 24, 2025.
25. Hergel, J., and Lefebvre, S., “Clean color: Improving multi-filament 3D prints”, *Computer Graphics Forum*, Vol. 33, Issue 2, 469-478, 2014.

26. Prasher, A., Shrivastava, R., Dahl, D., Sharma-Huynh, P., Maturavongsadit, P., Pridgen, T., Schorzman, A., Zamboni, W., Ban, J., Blikslager, A., Dellon, E. S., and Benhabbour, S. R., “Steroid Eluting Esophageal-Targeted Drug Delivery Devices for Treatment of Eosinophilic Esophagitis”, *Polymers*, Vol. 13, Issue 4, 1-20, 2021.
27. Catana, D. I., Pop, M. A., and Brus, D. I., “Comparison between Tests and Simulations Regarding Bending Resistance of 3D Printed PLA Structures”, *Polymers*, Vol. 13, Issue 24, 1-11, 2021.
28. Zohourkari, I., “Anisotropic Mechanical Properties of 3D Printed Poly-Lactic Acid Parts in the Plane Stress State”, *International Journal of Research Publication and Reviews*, Vol. 4, Issue 3, 4943-4948, 2023.
29. Syaefudin, E. A., Kholil, A., Hakim, M., Wulandari, D. A., Riyadi, and Murtinugraha, E., “The effect of orientation on tensile strength 3D printing with ABS and PLA materials”, *12th International Physics Seminar*, 1-7, Jakarta, 2023.
30. Spišák, E., Nováková-Marcinčinová, E., Nováková-Marcinčinová, L., Majerníková, J., & Mulidrán, P., “Investigation of the Manufacturing Orientation Impact on the Mechanical Properties of Composite Fiber-Reinforced Polymer Elements in the Fused Filament Fabrication Process”, *Polymers*, Vol. 15, Issue 13, 1-17, 2023.
31. Shen, Y., Lin, L., Wei, S., Yan, J., and Xu, T., “Research on the Preparation and Mechanical Properties of Solidified 3D Printed Concrete Materials”, *Buildings*, Vol. 12, Issue 12, 1-23, 2022.
32. Zaharin, H. A., Abdul Rani, A. M., Azam, F. I., Ginta, T. L., Sallih, N., Ahmad, A., Yunus, N. A., and Zulkifli, T. Z. A., “Effect of Unit Cell Type and Pore Size on Porosity and Mechanical Behavior of Additively Manufactured Ti6Al4V Scaffolds”, *Materials*, Vol. 11, Issue 12, 1-15, 2018.
33. Isaacson, N., Lopez-Ambrosio, K., Chubb, L., Waanders, N., Hoffmann, E., Witt, C., James, S., and Prawel, D. A., “Compressive properties and failure behavior of photocast hydroxyapatite gyroid scaffolds vary with porosity”, *Journal of Biomaterials Applications*, Vol. 37, Issue 1, 55-76, 2022.
34. Wolff, S., Lee, T., Faierson, E., Ehmann, K., and Cao, J., “Anisotropic properties of directed energy deposition (DED)-processed Ti-6Al-4V”, *Journal of Manufacturing Processes*, Vol. 24, 397-405, 2016.
35. von Windheim, N., Collinson, D. W., Lau, T., Brinson, L. C., and Gall, K., “The influence of porosity, crystallinity and interlayer adhesion on the tensile strength of 3D printed polylactic acid (PLA)”, *Rapid Prototyping Journal*, Vol. 27, Issue 7, 1327-1336, 2021.
36. Honda, S., Hashimoto, S., Nait-Ali, B., Smith, D. S., Daiko, Y., and Iwamoto, Y., “Characterization of anisotropic gas permeability and thermomechanical properties of highly textured porous alumina”, *Journal of the American Ceramic Society*, Vol. 105, Issue 10, 6335-6344, 2022.